Research Square

Preprints are preliminary reports that have not undergone peer review.
They should not be considered conclusive, used to inform clinical practice,
or referenced by the media as validated information.

Bayesian Spatio-Temporal Analysis of Malaria Risk under Climate Thresholds and Wetland Exposure in Rwanda

Similien Ndagijimana

similien.ndagijimana@rbc.gov.rw

Rwanda Biomedical Center

Aimable Mbituyumuremyi

Rwanda Biomedical Center

Clarisse Musanabaganwa

Rwanda Biomedical Center

Joel Gasan

Rwanda Biomedical Center

Alexis Manishimwe

Rwanda Biomedical Center

Ferdinand Maombi Maniriho

Rwanda Biomedical Center

Rhonah Umuriza

Rwanda Biomedical Center

Dunia Munyakanage

Rwanda Biomedical Center

Anastase Muhashyi

Rwanda Biomedical Center

Jean Damascene Niyonzima

Rwanda Biomedical Center

Epaphrdite Habanabakize

Rwanda Biomedical Center

Emmanuel Hakizimana

Rwanda Biomedical Center

Fausta Ndikumana

Ministry of Health

Christa Ishimwe

Ministry of Health

Thierry Sebakunzi

Ministry of Health
Valens Rwema
Ministry of Health
Samuel Nahimana
Ministry of Health
Jean de Dieu Harerimana
Ministry of Health
Emmanuel Ntawuyirusha
Ministry of Health
Patrick Niyonshuti
Ministry of Health
Josee Uwanyirigira
Ministry of Health
Adeline Umugwaneza
Ministry of Health
Piero Irakiza Mazimpaka
Ministry of Health
Theos Dieudonne Benimana
Ministry of Health
Espoir Mwungura Ngabo
Ministry of Health
Hassan Mugabo
Rwanda Biomedical Center
Christian Mazimpaka
Ministry of Health
Agnes Ikuzwe
University of Rwanda
Vedaste Iyakaremye
Rwanda Meteorological Service
Eric Remera
Rwanda Biomedical Center
Claude Mambo Muvunyi
Rwanda Biomedical Center

Article

Keywords: malaria, Rwanda, INLA, BYM2, wetland, marshland, climate thresholds, hotspot persistence, Anopheles arabiensis

Posted Date: September 25th, 2026

DOI: https://doi.org/10.21203/rs.3.rs-10729324/v1

License: This work is licensed under a Creative Commons Attribution 4.0 International License.
Read Full License

Additional Declarations: No competing interests reported.

Bayesian Spatio-Temporal Analysis of Malaria Risk under Climate Thresholds and Wetland Exposure in Rwanda

Similien Ndagijimana*[1], Aimable Mbituyumuremyi[2], Clarisse Musanabaganwa[1], Joel Gasana[1], Alexis Manishimwe[1], Ferdinand Maombi Maniriho[1], Rhonah Umuliza[1], Dunia Munyakanage[2], Anastase Muhashyi[2], Jean Damascene Niyonzima[2], Epaphrdite Habanabakize[2], Emmanuel Hakizimana[2], Fausta Ndikumana[3], Ishimwe Christa[3], Thierry Sebakunzi[3], Valens Rwema[3], Samuel Nahimana[3], Jean de Dieu Harerimana[3], Emmanuel Ntawuyirusha[3], Patrick Niyonshuti[3], Josée M Uwanyirigira[3], Adeline Umugwaneza[3], Piero Irakiza Mazimpaka[3], Theos Dieudonne Benimana[3], Espoir Mwungura Ngabo[3], Hassan Mugabo[1], Christian Mazimpaka[3], Agnes Ikuzwe[5], Vedaste Iyakaremye[4], Eric Remera[1], and Claude Mambo Muvunyi[6]

[1]Rwanda Biomedical Centre, Research, Innovation and Data Science Division, Kigali, Rwanda

[2]Rwanda Biomedical Centre, Malaria and Other Parasitic Disease Division, Kigali, Rwanda

[3]Ministry of Health, National Health Intelligence Centre, Kigali, Rwanda

[4]Rwanda Meteorological Agency, Kigali, Rwanda

[5]University of Rwanda, African Centre of Excellence in Data Science, Kigali, Rwanda

[6]Rwanda Biomedical Centre, Director General's Office, Kigali, Rwanda

September 10, 2026

Abstract

Background. Malaria transmission in Rwanda shows marked spatial heterogeneity and periodic resurgence despite sustained control efforts. The indepen-

*Corresponding author: similien.ndagijimana@rbc.gov.rw

dent contribution of sector-level wetland coverage to malaria incidence, after adjusting for lagged climate exposures and spatially structured random effects, has not previously been quantified. This study characterises the spatio-temporal dynamics of malaria across Rwanda, quantifies the dose-response relationship between wetland coverage and incidence, and evaluates competing Bayesian spatio-temporal models to identify the best-fitting framework for inference and public health planning.

Methods. Monthly malaria case data from all 416 administrative sectors (January 2014–December 2025; $n = 59{,}904$ sector-months) were obtained from the national HMIS. Sector-level wetland coverage (`swamp_prop`) was derived by intersecting a national swamp polygon layer (935 features) with sector boundaries. Bayesian spatio-temporal models were fitted in INLA under a Poisson likelihood, with climate covariates (ERA5-Land precipitation and humidity; MODIS NDVI) parameterised as 1-month-lagged categorical thresholds. Dose-response significance was assessed with Kruskal-Wallis and Spearman tests, and the spatio-temporal persistence of high-burden sectors was tracked across the 12-year window.

Results. Swamp proportion was the strongest independent landscape predictor of incidence (IRR = 1.18; 95% CrI: 1.08–1.28). Mean incidence rose from 31.4 per 1,000 in non-wetland sectors to 359.5 in high-wetland sectors ($H = 52.66$, $p < 0.001$). Heavy precipitation (>223 mm, lag 1; IRR = 1.10) and high humidity were positively associated with incidence, while low humidity (<60%) was protective (IRR = 0.89). The BYM2 mixing parameter ($\phi = 0.97$; 95% CrI: 0.86–1.00) showed that 97% of spatial variance was geographically structured. National incidence peaked at 448.2 per 1,000 in 2015, fell to 40.4 in 2023, and rose to 91.6 by 2025; 44 sectors sustained very high transmission (>100 per 1,000) in at least 10 of the 12 years, although none did so throughout all 12 years.

Conclusions. Wetland coverage independently predicts malaria incidence with a monotonic dose-response gradient. Persistently high-burden sectors cluster in marshland-dominated areas of Eastern Province and Kigali, supporting marshland-targeted interventions, larviciding, drainage, and agricultural water management within Rwanda's elimination strategy.

Keywords: malaria; Rwanda; INLA; BYM2; wetland; marshland; climate thresholds; hotspot persistence; *Anopheles arabiensis*

Background

Malaria has remained a major public health challenge in Rwanda throughout the twentieth and twenty-first centuries, advancing through distinct epidemiological phases shaped by the interplay of ecological, climatic, and programmatic factors. Sustained scale-up of insecticide-treated nets (ITNs), indoor residual spraying (IRS), and artemisinin-based combination therapy (ACT) between 2000 and 2012 achieved impressive declines in national incidence [2]. However, a pronounced resurgence between 2012 and 2018, among the largest documented in sub-Saharan Africa, demonstrated that these gains were fragile and that the drivers of malaria transmission in Rwanda operate through complex, non-linear mechanisms that simple intervention scale-up alone cannot fully address [2, 3]. Understanding and anticipating these dynamics at fine spatial and temporal resolution is essential for effective malaria programme planning.

Rwanda is administratively divided into 416 sectors across 30 districts, spanning a highly heterogeneous landscape from high-altitude montane areas (>2,000 m) in the North and Northwest to low-lying river valleys and marshlands in the East and South. This altitudinal gradient creates distinct malaria ecological zones in which transmission intensity is strongly stratified by elevation, vegetation, and proximity to water bodies [19, 3]. Prior Bayesian spatiotemporal analyses at the district level have confirmed substantial geographic heterogeneity in Rwanda's malaria burden, with persistently elevated relative risks concentrated in Eastern Province districts such as Bugesera, Kayonza, Ngoma, and Kamonyi in southern province and in Kigali's urban marshland districts [3, 26, 21, 4].

Wetland and marshland ecosystems are ecologically important drivers of malaria transmission. The dominant malaria vectors in Rwanda, *Anopheles arabiensis* and *An. gambiae s.s.*, require shallow, stagnant, or slow-moving water bodies for larval development over a period of 7-14 days [7]. Rwanda's lowland marshlands provide these conditions year-round, and the progressive conversion of natural papyrus-dominated wetlands into irrigated rice cultivation schemes, particularly in Bugesera, Gasabo, and Kayonza, has replaced a partially suppressive surface environment with warm, algae-rich, open-water microhabitats highly conducive to *Anopheles* larval survival [5, 6]. Despite this ecological plausibility, no prior study has formally quantified the independent contribution of sector-level wetland coverage to malaria incidence in Rwanda within a Bayesian spatio-temporal framework that simultaneously adjusts for lagged climate exposures and geographically structured random effects.

Climate variables govern malaria transmission through non-linear, threshold-dependent mechanisms that operate with a biological lag of 1-2 months, reflecting the combined

durations of mosquito larval development, adult emergence, and the extrinsic incubation period (EIP) of *Plasmodium falciparum*. Below approximately 18 °C, parasite sporogony arrests entirely; peak transmission efficiency occurs between 20 and 24 °C; above 34 °C, adult mosquito survival declines sharply [7]. Moderate rainfall creates optimal breeding habitat, while excessive precipitation can destroy shallow larval sites through flushing [14]. Relative humidity below 60% substantially reduces adult mosquito longevity and biting rate [13]. The emergence of partial artemisinin resistance mediated by *kelch13* (K13) R561H mutations, first confirmed in Rwanda and now documented across East Africa [22, 23, 24], and of pyrethroid resistance in primary vectors [25] further complicate the transmission environment and may contribute to renewed incidence increases in recent years.

Despite these well-established ecological and biological drivers, models for Rwanda have relied predominantly on linear or continuous climate representations applied at district level, without explicitly incorporating categorical threshold indicators or sector-level wetland covariates [3, 4]. This study addresses these gaps by analysing a comprehensive 12-year, sector-level monthly surveillance dataset spanning January 2014 to December 2025. It estimates the independent associations of wetland coverage, lagged climate thresholds, and geographic spatial structure with sector-level malaria incidence across Rwanda.

Methods

Study design and data

A retrospective ecological design was used. Monthly malaria case counts from all 416 sectors (January 2014–December 2025; $n = 59{,}904$ sector-months) were obtained from the national HMIS/DHIS2. Population denominators, from NISR projections, served as model offsets. Climate variables such as maximum/minimum temperature, precipitation, relative humidity and NDVI were extracted from the ERA5-Land reanalysis and MODIS and aggregated to the sector-month level. Sector- level wetland coverage (`swamp_prop`) was derived by spatial intersection of a nationally validated swamp polygon layer (SwampFinal.shp; 935 features; Transverse Mercator CRS, reprojected to WGS84) with the NISR sector boundary shapefile, yielding the ratio of swamp area to total sector area, standardised to unit standard deviation prior to modelling.

Climate threshold parameterisation

To capture non-linear climate–malaria relationships, climate variables were categorised into epidemiologically motivated thresholds and incorporated as 1-month lagged indi-

cators. The choice of each threshold was guided by established biological evidence:

- **Temperature (lag 1): <18.5 °C; 18.5–23.9 °C (reference); >23.9 °C.** The lower bound of 18.5 °C reflects the minimum temperature below which *Plasmodium falciparum* sporogony arrests and vectorial capacity effectively reaches zero, as quantified by mechanistic thermal performance models [7]. The upper bound of 23.9 °C approximates the transition point above which parasite development may accelerate beyond the duration sustainable by remaining adult mosquito lifespan.

- **Precipitation (lag 1): <73 mm; 73–223 mm (reference); >223 mm.** These boundaries correspond to the lower and upper tertiles of the observed sector-month rainfall distribution in this dataset. The lower category (<73 mm) represents conditions likely insufficient for sustained larval habitat formation; the upper category (>223 mm) captures intense rainfall that may produce stagnant surface water in low-lying wetland areas but can also destroy shallow breeding sites through flushing [14].

- **Relative humidity (lag 1): binary <60% vs ≥60% (reference).** The 60% threshold is derived from published evidence that adult *Anopheles* daily survival probability declines substantially below this level, reducing mosquito longevity and biting rate below values needed to sustain transmission cycles [13].

- **Season:** short dry (January–February; reference); long rainy (March–May); long dry (June–August); short rainy (September–December).

A 1-month lag was selected *a priori* based on the combined biological delay of approximately 28–35 days encompassing larval development, adult emergence, and the *P. falciparum* extrinsic incubation period [8].

Bayesian spatiotemporal model

Let $y_{s,t}$ denote observed malaria cases with expected cases $E_{s,t}$:

$$y_{s,t} \sim \text{Poisson}(\mu_{s,t}) \tag{1}$$

$$\log(\mu_{s,t}) = \log(\mathit{population}_{s,t}) + \alpha + \boldsymbol{X}_{s,t}\boldsymbol{\beta} + u_s + v_s + \gamma_t + \delta_{s,t} \tag{2}$$

where $\log(\text{population}_{s,t})$ is the population offset, $\boldsymbol{X}_{s,t}\boldsymbol{\beta}$ includes lagged climate thresholds, seasonal indicators, NDVI (lag 1), and `swamp_prop`; u_s and v_s are the structured and unstructured spatial components mixed via the BYM2 parameterisation through ϕ; γ_t is a first-order random walk (RW1) temporal trend; and $\delta_{s,t}$ is an IID space-time interaction term. We used the scaled BYM2 parameterisation [10], in which the mixing parameter $\phi \in [0, 1]$ quantifies the proportion of spatial variance attributable to

geographic structure. Penalised complexity (PC) priors [11] were assigned as follows: $P(\sigma > 1) = 0.01$ for all precision hyperparameters, and $P(\phi < 0.5) = 0.5$. All models were fitted using R-INLA [12] and evaluated using WAIC, DIC, and mean $-\log$ CPO.

Dose-response and persistence analyses

Sectors were classified into four wetland exposure categories: non- wetland (`swamp_prop` = 0), low (0-5%), moderate (5-20%), and high (>20%). Statistical significance of the wetland-incidence gradient was assessed using Kruskal-Wallis H test (four categories) and Spearman rank correlation (continuous `swamp_prop`). Sector- level persistence of high malaria burden was assessed by counting the number of years (out of 12) in which annual incidence exceeded 100 cases per 1,000 population. Sectors were classified as high persistence (≥7 of 12 years), very high persistence (≥10 of 12 years), or persistently high-transmission sectors (above threshold in all 12 years) throughout.

Results

National temporal trend (2014–2025)

Figure 1 presents the national malaria incidence trajectory. From a baseline of 293.8 per 1,000 in 2014, incidence surged to a peak of 448.2 per 1,000 in 2015, remaining heavily elevated through 2017 (432.0 per 1,000). A sustained multi-year decline followed, driven by intensified ITN distribution, expanded IRS coverage, and the roll-out of pyrethroid-PBO nets, reaching a historic minimum of 40.4 per 1,000 in 2023. Crucially, incidence then rebounded to 91.6 per 1,000 by 2025, a 127% increase over two years that departs from the downward linear trend, signalling new programmatic challenges.

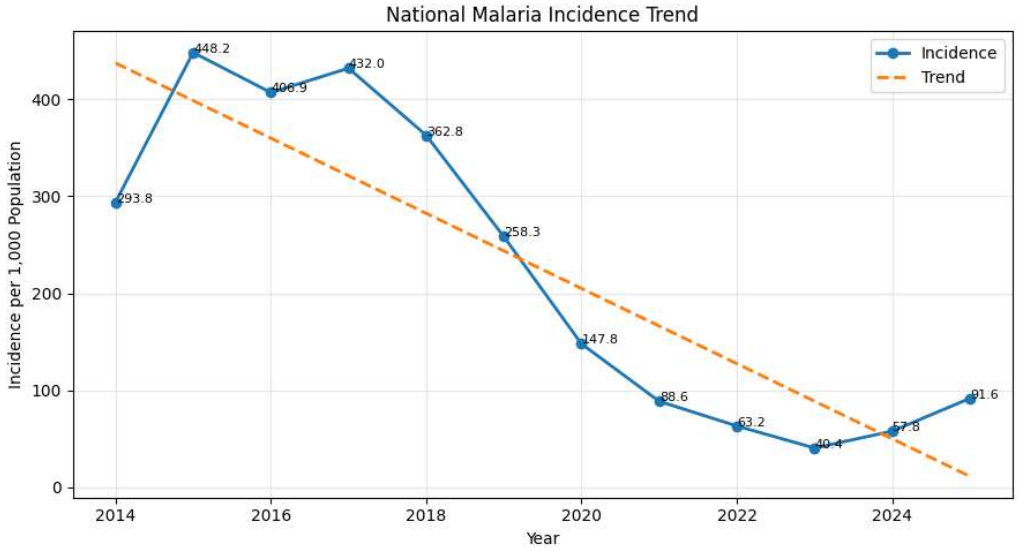


Figure 1: National malaria incidence trend in Rwanda, 2014–2025. Points represent annual mean incidence per 1,000 population. Annotated values indicate annual incidence. The dashed orange line shows the long-term linear trend; the 2023–2025 rebound departs markedly from this trajectory.

Bayesian posterior temporal relative risk (RW1 effect)

Figure 2 shows the posterior mean relative risk (RR) and 95% credible interval derived from the RW1 temporal random effect of the selected BYM2 threshold model. This figure is qualitatively distinct from Figure 1: rather than showing raw incidence counts, it isolates the smooth temporal signal in the model after accounting for all fixed climate and landscape covariates, spatial random effects, and seasonal patterns. Three temporal phases are clearly delineated.

Phase I: Resurgence (2014-2018): Posterior mean RR peaked at approximately RR ≈ 7–8 around January 2016, with high temporal variability throughout 2015-2018 (RR oscillating between 2 and 7) and wide 95% credible intervals, reflecting genuine epidemiological uncertainty during the malaria resurgence period. This extreme RW1 signal implies that beyond what climate thresholds and landscape covariates explain, a large residual unexplained temporal amplification occurred during this phase, consistent with insecticide and drug resistance emergence [23, 24].

Phase II: Decline (2019–2021): Posterior mean RR declined sharply across 2019–2020, crossing the RR $= 1$ null line in mid-2020 and stabilising below unity through 2020–2024. The narrowing credible intervals in this phase indicate greater temporal stability and reduced residual variation, consistent with the documented effectiveness of intensified national vector control and improved case management [18, 1].

Phase III: Emerging rebound (2024–2025): A subtle but consistent upward inflection is visible from 2024, with posterior mean RR approaching 0.5–0.7. While still below the

RR = 1 threshold, the upward trajectory is statistically distinguishable from the 2021–2023 nadir, providing early model-based evidence of renewed temporal amplification in malaria risk beyond what the fixed climate effects capture. This signal corroborates the raw incidence rebound (Figure 1) and reinforces the programmatic urgency of investigating non-climatic drivers including partial artemisinin resistance [22, 23] and pyrethroid resistance [1, 25].

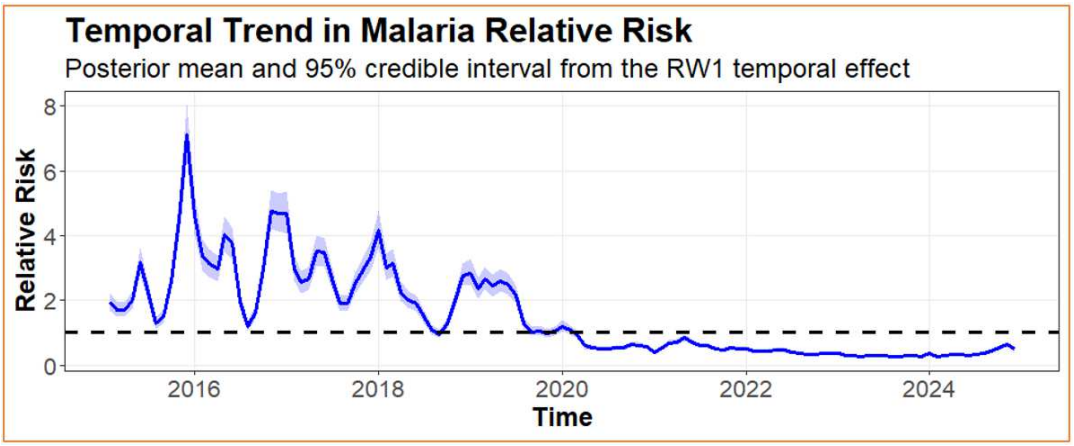


Figure 2: Posterior temporal trend in malaria relative risk from 2014-2025

Seasonal profile

Figure 3 shows the pooled monthly incidence profile across all sectors and years. A classic bimodal transmission pattern is observed, closely synchronised with Rwanda's rainfall calendar. The primary peak reaches 318 per 1,000 in December, sustained into January (294 per 1,000), reflecting the short rainy season (September– November) incubation lag. A secondary peak of 235 per 1,000 occurs in June, following the long rainy season (March–May). The annual trough of 109 per 1,000 falls in August at the height of the long dry season. This bimodal pattern provides a strong basis for the timing of seasonal preventive interventions, with IRS campaigns and LLIN distribution optimally deployed before October and before February to precede the dual transmission peaks.

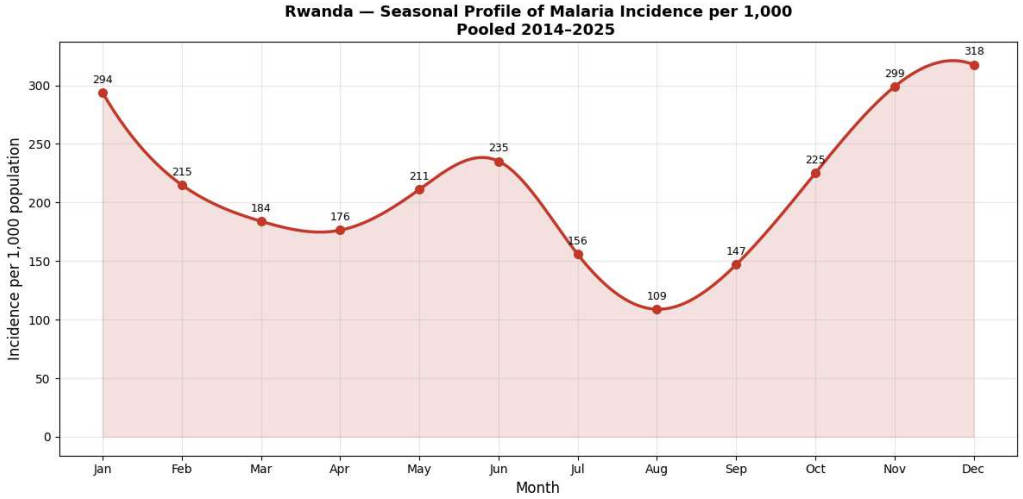


Figure 3: Pooled seasonal profile of malaria incidence per 1,000 population, Rwanda 2014–2025.

Geographic distribution of malaria burden

Figure 4 maps mean sector-level malaria incidence over the 12-year study period. Against a national mean of 218.6 per 1,000, the geographic distribution reveals profound eco-zonal polarisation. The highest-burden quintile (Q5: 408–1,462 per 1,000) forms a contiguous hyper-endemic belt spanning the Eastern Province, particularly Kayonza, Gatsibo, and Bugesera districts, and extends into the low-altitude river valleys of the Southern Province (Huye, Gisagara, and Nyanza). This pattern closely mirrors the distribution of sector-level wetland coverage, with wetland sectors recording a mean of 229.1 per 1,000 versus 31.4 per 1,000 in non-wetland sectors (7.3-fold disparity). Conversely, the high-altitude Northern Province (Musanze, Nyabihu, Burera) functions as a low-transmission refugium (Q1: 2–20 per 1,000), where conditions are consistently sub-optimal for vector survival and parasite development. Kigali's urban marshland districts (Gasabo, Kicukiro) constitute an anomalously high-burden urban pocket, driven by irrigated vegetable and rice farming within the city's wetland blocks.

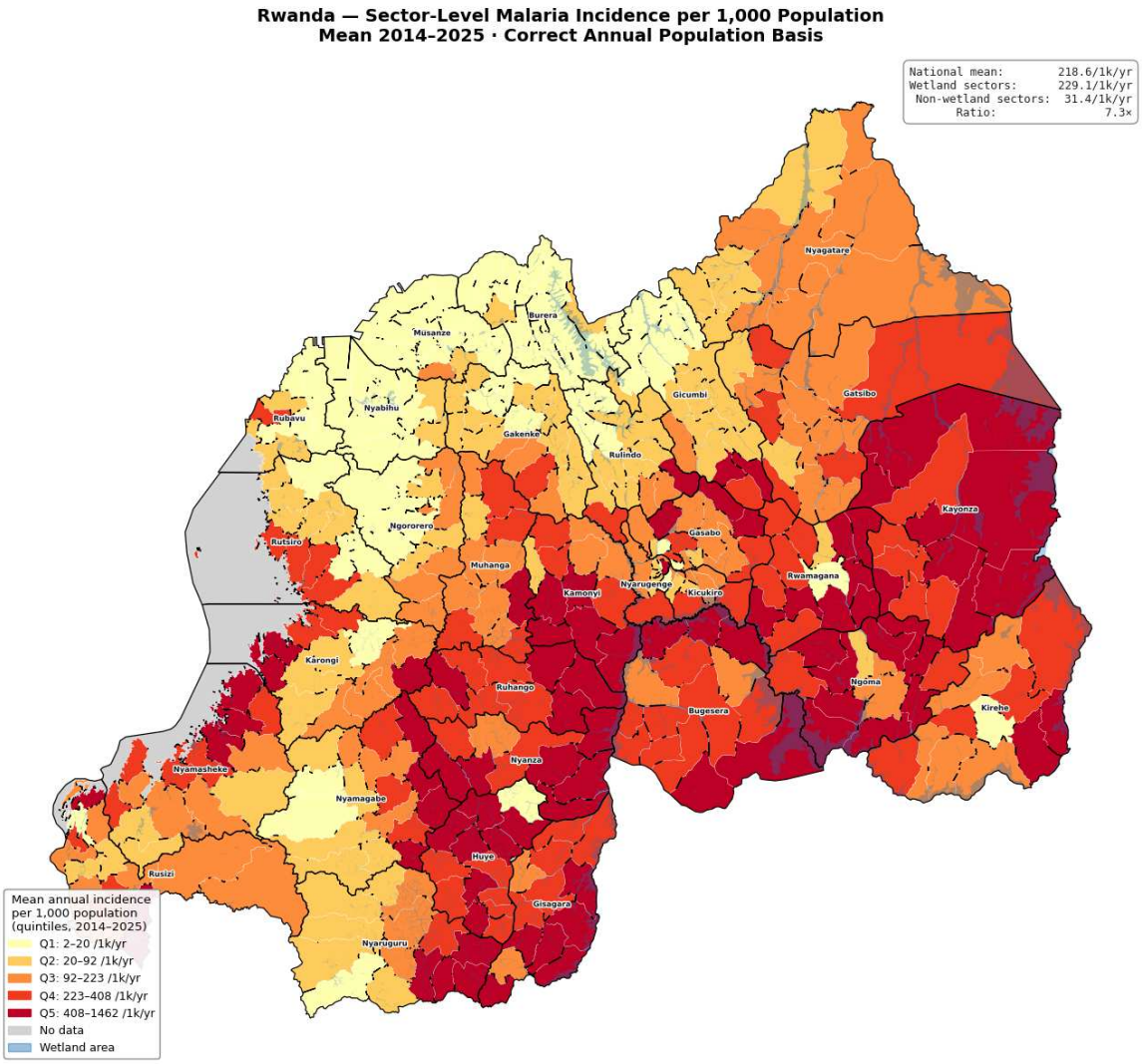


Figure 4: Mean sector-level malaria incidence per 1,000 population per year, Rwanda 2014–2025.

Spatiotemporal persistence of hotspots

Figure 5 maps the number of years (out of 12) in which each sector exceeded 100 cases per 1,000 population. A total of 134 sectors exhibited high persistence ($\geq$7 of 12 years), and 44 sectors reached very high persistence ($\geq$10 of 12 years), indicated by white outlines; no sector exceeded the threshold in every study year (12/12 years) in this updated analysis. These very high-persistence sectors are concentrated in three geographic clusters.

Cluster 1: Central-to-southern corridor. Very high-persistence sectors span Kamonyi, Ruhango, Gisagara, and Huye districts, including Kansi (558 per 1,000), Gishubi (648 per 1,000), Muganza (550 per 1,000), and Nyanza (461 per 1,000). These are lowland sectors characterised by rice-growing river valleys and irrigated marshland.

Cluster 2: Eastern Province Akagera zone. The lacustrine marshland zones of Buge-

sera include Kamabuye (673 per 1,000) and Rweru (464 per 1,000), sustained by year-round surface water from Lake Cyohoha and the Akagera river system.

Cluster 3: Western Province Lake Kivu shoreline (Karongi and Nyamasheke districts). A third, geographically distinct cluster is evident along the western border, comprising sectors in Karongi district (including Mubuga 798 per 1,000, Gihombo 559 per 1,000, and Gishyita 619 per 1,000) and several sectors in Nyamasheke district. These sectors show very high persistence (10–11 years out of 12 in the darkest remaining categories), despite being in the Western Province which is generally considered lower-burden. Their elevated persistence is associated with the extensive aquatic vegetation belts fringing Lake Kivu at altitudes of 1,460– 1,600 m, which provide year-round *Anopheles* larval habitat at temperatures that remain within the transmission-permissive range. Unlike the Eastern Province clusters, these sectors are not characterised by irrigated rice cultivation but by natural wetland margins, suggesting that the wetland-incidence association identified in the Bayesian model captures both irrigated and natural wetland types. Additionally, Rutsiro district, in the northern Western Province, contains isolated sectors with moderate-to-high persistence (4–9 years), consistent with its lowland lake-margin position.

The Northern Province (Musanze, Nyabihu, Burera, Gakenke) remains almost entirely at zero persistence across all 12 years, reflecting the thermal barrier at high altitude (>2,000 m) where temperatures are consistently below the transmission-permissive threshold. The spatial pattern across all three clusters (Eastern lowland marshlands, central-southern river valleys, and Western Province lake margins) is consistent with a common ecological mediator: proximity to permanent or semi-permanent surface water bodies that support year-round *Anopheles* breeding, regardless of land-use type.

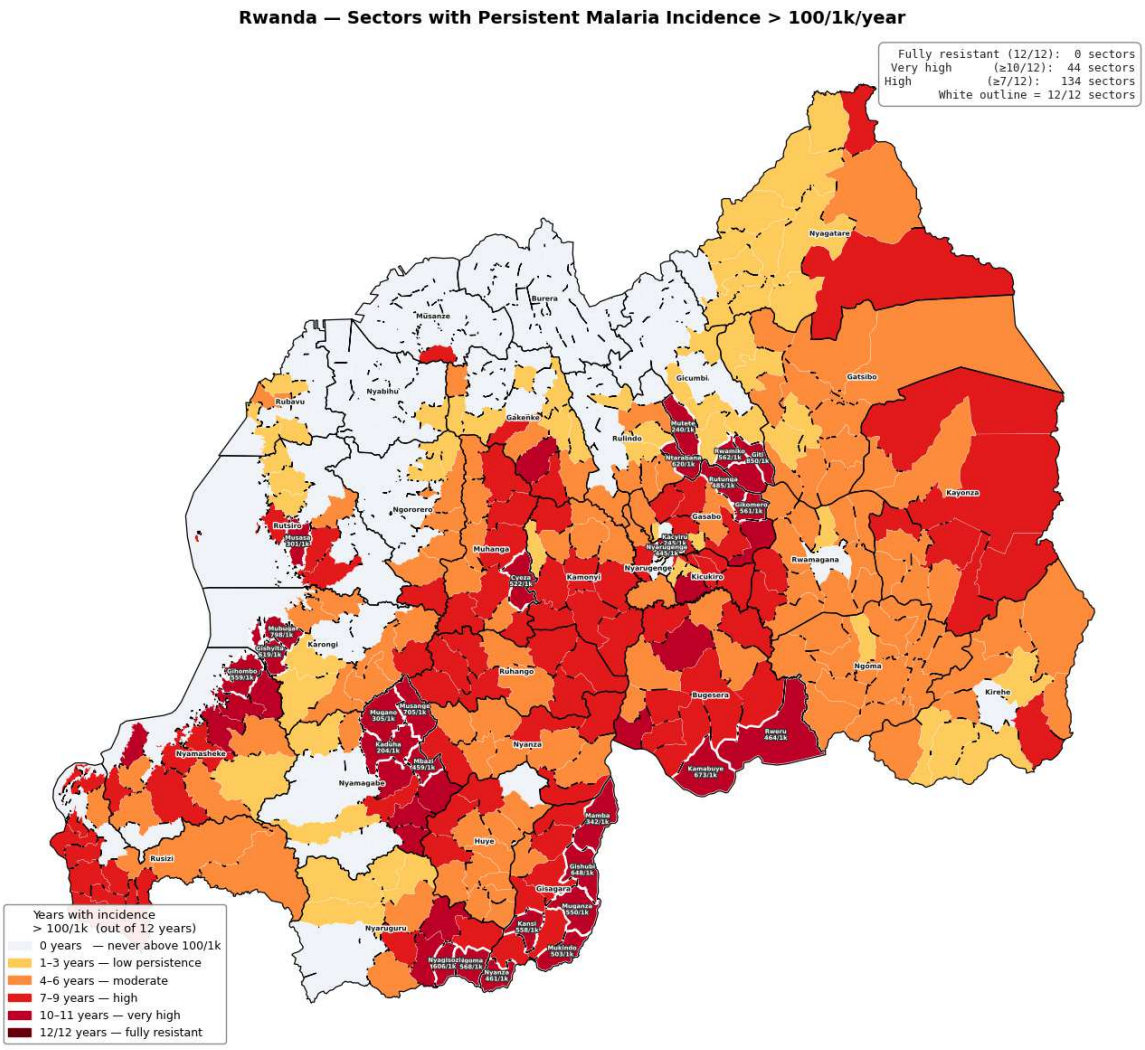


Figure 5: Spatiotemporal persistence of malaria incidence >100 cases per 1,000 population per year across Rwanda sectors, 2014–2025. Colour scale represents number of years out of 12 above the threshold. Sectors with white outlines (44 in total) reached very high persistence (≥10 of 12 years); no sector exceeded the threshold in all 12 years in this updated analysis. A total of 134 sectors reached high persistence (≥7 of 12 years). Sector-specific incidence values are labelled for selected high-burden sectors. Districts are labelled in black.

Fixed-effect posterior estimates

Table 1 presents posterior estimates from the selected BYM2 threshold model. Swamp proportion was the strongest independent fixed-effect predictor across all BYM2 specifications (IRR = 1.18; 95% CrI: 1.08–1.28), consistent across the concurrent climate model (IRR = 1.19; 95% CrI: 1.08–1.30). Heavy precipitation (>223 mm, lag 1) increased malaria incidence by 10% (IRR = 1.10; 95% CrI: 1.07–1.14). Low relative humidity (<60%) was protective (IRR = 0.89; 95% CrI: 0.86–0.93). The long rainy season (March–May) was paradoxically associated with lower incidence relative to the short dry season reference (IRR = 0.83; 95% CrI: 0.73–0.94). The BYM2 spatial mixing parameter $\phi = 0.97$ (95% CrI: 0.86–1.00) confirmed that 97% of spatial variance

was geographically structured.

Table 1: Fixed-effect posterior estimates: BYM2 threshold model (selected). Reference categories: temperature 18.5–23.9 °C; precipitation 73–223 mm; relative humidity ≥60%; season = short dry. IRR = Incidence Rate Ratio; CrI = credible interval.

Variable	Category	IRR	95% CrI	Interpretation
Temperature (lag 1)	<18.5 °C	2.78	0.21–12.23	Uncertain
Precipitation (lag 1)	<73 mm	1.00	0.97–1.03	No significant effect
	>223 mm	**1.10**	**1.07–1.14**	Increased risk
Relative humidity (lag 1)	<60%	**0.89**	**0.86–0.93**	Protective
Season	Long dry	0.93	0.80–1.07	Not significant
	Long rainy	**0.83**	**0.73–0.94**	Lower risk
	Short rainy	1.07	0.94–1.21	Not significant
NDVI (lag 1, scaled)	Continuous	1.01	1.00–1.03	Marginal positive
Swamp prop. (scaled)	**Continuous**	**1.18**	**1.08–1.28**	**Strongest landscape predictor**

Wetland dose-response

Table 2 shows the monotonic dose-response gradient. Mean annual incidence rose from 31.4 per 1,000 in non-wetland sectors to 359.5 per 1,000 in sectors with >20% wetland coverage. Notably, even minimal wetland coverage (0–5%) was associated with mean incidence of 186.5 per 1,000, nearly six times that of non-wetland sectors, suggesting that marshland effects operate at low exposure thresholds. The gradient was statistically robust across all frameworks applied (Kruskal-Wallis $H = 52.66$, $p = 2.2 \times 10^{-11}$; Spearman $\rho = 0.38$, $p < 0.001$).

Table 2: Dose-response relationship between sector-level wetland coverage and mean annual malaria incidence, Rwanda 2014–2025.

Wetland category	N sectors (%)	Mean	Median
Non-wetland (`prop` = 0)	22 (5.3%)	31.4	11.1
Low (0–5%)	230 (55.3%)	186.5	112.3
Moderate (5–20%)	142 (34.1%)	277.9	226.6
High (>20%)	22 (5.3%)	**359.5**	**342.2**

Kruskal-Wallis $H = 52.66$, $p = 2.2 \times 10^{-11}$; Spearman $\rho = 0.38$, $p < 0.001$.

Discussion

This study provides the first sector-level Bayesian spatiotemporal analysis of malaria in Rwanda that formally estimates the association between wetland coverage and malaria incidence after adjustment for lagged climate, seasonal variation, vegetation greenness, and geographically structured random effects. Swamp proportion (IRR = 1.18; 95% CrI: 1.08–1.28) was the strongest independent predictor of malaria incidence across all BYM2 specifications, a finding robust to full covariate adjustment. This advances over prior unadjusted ecological correlations is important: it indicates that the wetland–incidence association is not attributable to confounding by climate or seasonal factors, but the observational ecological design prevents causal inference and residual confounding by unmeasured factors cannot be excluded.

The 11-fold dose-response gradient between non-wetland and high-wetland sectors (Table 2, Figure 4) and the measurable association even at minimal coverage (0–5%) are consistent with Van Hullebusch et al. [5], who documented elevated *Anopheles* vector density in rice-farming communities in Bugesera, and with evidence from West Africa linking irrigated agriculture to micro-geographic malaria heterogeneity [9]. The estimated 15–19% difference in incidence per standard deviation increase in swamp proportion is comparable in magnitude to the effect of targeted IRS campaigns, suggesting that environmental management of wetlands may represent a meaningful complementary approach. Rwanda Biomedical Centre's drone-based *Bti larviciding* programme in Gasabo [6] provides a proof-of-concept; prospective evaluation of the effectiveness of scaling environmental management to high-wetland sectors would be informative.

The BYM2 threshold model confirms that malaria transmission in Rwanda operates through ecological suitability windows rather than monotonic climate effects, consistent with the temperature optimum of 20–24 °C identified by Mordecai et al. [7]. Heavy rainfall (>223 mm, lag 1; IRR = 1.10) expanded breeding habitat in low-lying wetland sectors, while low relative humidity (<60%; IRR = 0.89) reduced adult mosquito longevity, reflecting humidity-dependent survival mechanisms documented by Yamana and Eltahir [13]. The protective effect of very high rainfall (>223 mm) observed in heatmap exploratory analyses is consistent with flushing effects that destroy shallow larval habitats [14]. The 1-month lag specifications outperformed concurrent models by WAIC differences exceeding 3,600 units, confirming the biological importance of the larval development EIP delay chain [8, 15].

The paradoxical association of the long rainy season (March–May) with lower incidence (IRR = 0.83) relative to the short dry season warrants careful interpretation. Three mechanisms likely contribute: (i) vector washout, in which intense long-rains

precipitation destroys shallow breeding sites through flushing [14]; (ii) a healthcare-seeking reporting lag, in which peak-season cases are counted in the subsequent month, shifting their apparent timing toward the short dry season; and (iii) dilution of breeding site suitability when total rainfall exceeds the optimal threshold. The seasonal profile (Figure 3), with a December peak and June secondary peak that is temporally consistent with 1–2 month lags after the short and long rainy seasons, respectively, supporting mechanism (ii). These patterns have direct operational implications: IRS campaigns should be deployed before October and before February, ahead of the dual incidence peaks, consistent with NMCP programme timing guidance.

The BYM2 mixing parameter $\phi = 0.97$ (Table 1) demonstrates that virtually all spatial variance in malaria incidence is geographically structured rather than random, a level of spatial autocorrelation exceptionally high even by sub-Saharan African malaria mapping standards [3, 4]. This finding validates the BYM2 modelling choice over simpler regression approaches: had spatial autocorrelation been ignored, fixed-effect standard errors would have been substantially underestimated and IRR estimates biased. The geographic coherence of the hyper-endemic belt (Figure 4), spanning the Eastern Province and extending into the southern river valleys, implies that high-risk sectors are ecologically contiguous rather than randomly scattered, favouring geographically targeted, coordinated intervention packages over sector-by-sector programmes.

The 12-year national trajectory (Figure 1) and the Bayesian posterior RW1 temporal signal (Figure 2) together reveal malaria dynamics not consistent with simple programmatic success or failure narratives. The RW1 posterior separates residual temporal variation from climate and landscape effects: the resurgence phase (2014–2018; peak RR $\approx$7–8 in early 2016) corresponds to documented co-occurrence of *kelch13* R561H partial artemisinin resistance emergence in Rwanda [22, 23], pyrethroid resistance reducing ITN and IRS efficacy [25], and funding gaps, though attribution from observational data alone is not possible. The decline phase (2019–2024), in which the RW1 posterior crosses RR = 1 in mid-2020 and stabilises below unity with narrow credible intervals, is contemporaneous with scale-up of pyrethroid-PBO nets and intensified case management [18]. The post-2024 upward inflection in the RW1 posterior remains modest (RR approaching but below 1), yet the parallel rise in raw incidence to 91.6 per 1,000 by 2025 warrants investigation; potential contributing mechanisms include escalating K13 mutation prevalence [24], cross-border parasite importation [23], and pyrethroid resistance intensity escalation [25], but these hypotheses cannot be evaluated with surveillance data alone and require entomological and genomic monitoring.

The 44 sectors classified as very high persistence ($\geq$10 of 12 years; Figure 5) represent a distinct epidemiological challenge from the broader high-burden caseload; none reached full 12/12-year persistence in this updated analysis. The Eastern Province

clusters (Kamabuye 673 per 1,000; Rweru 464 per 1,000 in Bugesera; and the central-southern corridor including Kansi 558 per 1,000 and Gishubi 648 per 1,000) have been previously documented in district-level analyses [21, 4]. However, the Lake Kivu shoreline cluster in Karongi and Nyamasheke districts of the Western Province (with sectors such as Mubuga 798 per 1,000, Gihombo 559 per 1,000, and Gishyita 619 per 1,000 maintaining very high persistence across 10–11 years) represents an ecologically distinct high-burden zone that has received less programmatic attention. These Western Province sectors are not characterised by irrigated rice agriculture but by natural papyrus and aquatic macrophyte belts along the Lake Kivu shoreline at elevations of approximately 1,460–1,600 m. The fact that persistence is near-equivalent to the Eastern lowland clusters despite cooler temperatures suggests that the permanence and extent of the shoreline wetland habitat compensates for thermal constraint, sustaining vectorial capacity year-round. This finding extends the wetland–incidence association beyond irrigated agriculture to encompass natural lacustrine wetlands, and implies that the swamp proportion covariate in the model captures both land-use types.

The concentration of all three geographic clusters in the highest wetland coverage quintile is consistent with landscape exposure as a contributing factor to chronic high transmission, though causal attribution is not warranted from this ecological study design. These sectors may function as epidemiological reservoirs that sustain parasite and vector populations during national low-transmission periods [17]; prospective entomological investigation is needed to evaluate this hypothesis.

Environmental management approaches, including targeted larviciding, drainage, and agricultural water management [5], may be particularly relevant in these structurally entrenched sectors. For the Western Province lake-margin cluster specifically, approaches that can be applied to natural wetland margins (such as biological larviciding with Bti) rather than drainage or land-use change may be more feasible and ecologically appropriate. The effectiveness of such interventions at scale has not yet been formally evaluated and warrants prospective study.

This study extends four prior Bayesian spatiotemporal analyses of malaria in Rwanda. Semakula et al. (2020) [3] applied BYM models at district level using annual aggregated data (2012–2018) and identified elevated relative risks in Eastern Province but did not incorporate wetland covariates, lagged climate parameterisation, or threshold effects. Semakula et al. (2023) [26] integrated DHS survey and HMIS routine data within a spatiotemporal framework at district resolution without dose-response characterisation of landscape exposures. Semakula et al. (2024) [4] extended demographic stratification across three age-sex groups (children under 5, adult males, adult females), identifying Kamonyi, Ngoma, Kayonza, and Bugesera as persistently high-burden districts, but similarly did not quantify the marshland effect independently. Rubuga et al. (2024)

[21] applied BYM2 and SaTScan scan statistics to the 2012–2022 dataset across 30 districts, confirming elevated relative risks and geographic clustering but at district rather than sector resolution and without wetland covariates or climate threshold parameterisation. Nzabakiriraho and Gayawan [16] applied geostatistical modelling to malaria prevalence among under-five children but at a cross-sectional scale without temporal dynamics.

The present study advances this body of evidence in six dimensions: (i) sector-level analysis (416 units vs. 30 districts), providing substantially greater spatial resolution; (ii) formal inclusion of sector-level wetland coverage as an independent fixed-effect covariate; (iii) BYM2 parameterisation enabling direct inference on the spatial mixing parameter ϕ; (iv) categorical climate threshold parameterisation grounded in biological mechanisms; (v) a 12-year hotspot persistence analysis identifying structurally entrenched reservoirs; and (vi) the RW1 posterior temporal visualisation (Figure 2) that separates structural temporal dynamics from climate-driven variation and provides an early warning tool for programme managers.

Strengths and limitations

Strengths. This study benefits from a 12-year, near-complete monthly surveillance dataset from all 416 sectors of Rwanda ($n = 59{,}904$ sector-months), providing substantial statistical power for spatiotemporal inference. The BYM2 model with PC priors represents current best practice for disease mapping [10, 11]. Integration of a nationally validated swamp polygon layer with sector-level spatial intersection provides a geographically precise landscape covariate not previously available in Rwanda malaria models. The multi-model comparison framework spanning six competing specifications ensures that the primary findings are empirically justified.

Limitations. First, this is an observational ecological study: associations are reported throughout and should not be interpreted causally; residual confounding by unmeasured factors such as healthcare access, housing quality, ITN use behaviour cannot be excluded. Second, HMIS passive surveillance undercounts true incidence and varies in reporting completeness across sectors and years; temporal changes in Figure 1 may partly reflect improvements in diagnostic coverage or reporting practices. Third, the time-invariant wetland covariate does not capture progressive land-use change, notably the ongoing conversion of natural marshland to irrigated rice cultivation, over the study period. Fourth, sector-level ITN coverage, IRS programme reach, and community health worker density were unavailable at the sector-month level and could not be included as covariates, potentially confounding climate and landscape effect estimates. Fifth, the temperature category below 18.5 °C was represented by a single sector-month, rendering that threshold estimate unreliable and precluding interpreta-

tion.

Conclusion

Bayesian spatiotemporal analysis of malaria across Rwanda's 416 sectors from 2014 to 2025 identifies wetland coverage as the strongest independent ecological predictor of malaria incidence after full covariate adjustment, with a monotonic 11-fold dose-response gradient across wetland coverage categories. The dominance of geographically structured spatial variance ($\phi = 0.97$), meaning that sector location rather than random variation accounts for nearly all spatial heterogeneity in malaria risk, confirms that malaria in Rwanda is ecologically entrenched. Forty-four sectors reaching very high persistence ($\geq$10 of 12 years), concentrated in marshland-dominated areas of the Eastern Province and Kigali, sustained incidence above 100 per 1,000 in nearly every study year, though none did so in all 12 years, suggesting these areas may benefit from locally intensified intervention approaches. The post-2023 incidence rise warrants entomological and genomic surveillance to identify its mechanisms. These findings support evaluation of marshland-targeted environmental management as a component of Rwanda's elimination strategy and highlight the value of sector-level spatiotemporal modelling for climate-informed malaria surveillance [20].

Research and programme implications:

1. Wetland coverage was independently associated with malaria incidence; prospective evaluation of targeted environmental management, such as including larviciding and drainage in the 75 sectors with >10% swamp coverage and the 44 sectors reaching very high persistence ($\geq$10 of 12 years), is warranted.
2. The bimodal seasonal profile supports timing of preventive interventions before November–December and May–June transmission peaks, accounting for the 1–2 month climate–incidence lag.
3. The 44 sectors reaching very high persistence ($\geq$10 of 12 years) merit evaluation for locally intensified intervention strategies.
4. The post-2023 incidence rebound, not attributable to fixed climate effects, should be investigated through entomological insecticide resistance surveillance and genomic parasite monitoring for artemisinin partial resistance.
5. Integration of sector-level spatiotemporal INLA models into DHIS2 warrants evaluation as a real-time, climate-informed early warning tool.

Declarations

Funding. No specific funding was received for this review. The authors are employed by the Rwanda Biomedical Centre and the Ministry of Health, Kigali, Rwanda, whose mandates encompass climate-health preparedness. The funders had no role in the preparation of this manuscript.

Competing interests. The authors declare that they have no competing interests.

Data availability. The health data supporting the findings of this study were obtained from the Rwanda Ministry of Health (MoH) and are not publicly available due to data governance and confidentiality requirements. Access may be granted upon reasonable request to the corresponding author, subject to approval by the data custodian. ERA5-Land climate data are publicly available from the ECMWF Copernicus Climate Change Service (https://cds.climate.copernicus.eu). Spatial boundary and population data are available from NISR (https://www.statistics.gov.rw).

Ethical Considerations. This study is a secondary analysis of routinely collected, aggregate, sector-level malaria surveillance data; no individual patient records, personal identifiers, or direct contact with human subjects were involved at any stage of the research. Access to and use of the data were authorised by the Rwanda Ministry of Health (MoH), the data custodian, in accordance with national health-data governance and confidentiality requirements. Because the dataset contained no individually identifiable information and the analysis involved no direct engagement with human participants, formal institutional ethics committee review was not sought for this study. As no individual-level data were collected or used, informed consent was not applicable.

Author contributions. SN: Conceptualisation, Methodology, Formal analysis, Data curation, Investigation, Visualisation, Writing original draft, Writing review and editing, and Correspondence. ER: Conceptualisation, Methodology, Supervision, Project administration, Writing review and editing. CMM: Conceptualisation, Supervision, Writing review and editing.CM, JG, AM, FN, AMu, BM, FM, RU, AI, IC, TS, VR, SNa, JDH, EN, PN, MJU, AU, PIM, TDB, EMN, HM, DM, JDN, EH, EHa, AMb, and DH contributed to data acquisition, literature review, interpretation of findings, critical revision of the manuscript, and approved the final version for publication. All authors reviewed and approved the final manuscript and agree to be accountable for all aspects of the work.

References

[1] World Health Organisation. World Malaria Report 2024. WHO, Geneva, 2024. https://www.who.int/teams/global-malaria-programme/reports/world-malaria-report-2024

[2] Karema, C., Wen, S., Sidibe, A., Smith, J.L., Gosling, R., Hakizimana, E., Tanner, M., Noor, A.M., & Tatarsky, A. History of malaria control in Rwanda: implications for future elimination. *Malaria Journal*, 19(1):356, 2020. DOI: 10.1186/s12936-020-03407-1

[3] Semakula, M., Niragire, F., & Faes, C. Bayesian spatio-temporal modelling of malaria risk in Rwanda. *PLOS ONE*, 15(9):e0238504, 2020. DOI: 10.1371/journal.pone.0238504

[4] Semakula, M., Tuyishime, P., & Niragire, F. Spatio-temporal dynamics of malaria in Rwanda between 2012 and 2022. *Infectious Diseases of Poverty*, 13(1):71, 2024. DOI: 10.1186/s40249-024-01237-w

[5] Van Hullebusch, E.D., Franke, A.C., Nijenhuis, R.C., Dossou-Yovo, E.R., & Struik, P.C. Local resource mobilisation for malaria vector control among Rwandan rice farmers. *Journal of Health, Population and Nutrition*, 42(1):37, 2023. DOI: 10.1186/s41043-023-00345-x

[6] Hakizimana, E., Karema, C., Munyakanage, D., Githure, J., Mazur, C., & Tongren, J.E. Factors affecting community participation in drone-based larviciding using *Bacillus thuringiensis israelensis* for bio-control of malaria vectors in Rwanda. *Parasites & Vectors*, 2025. PMC11872309.

[7] Mordecai, E.A., Paaijmans, K.P., Johnson, L.R., et al. Optimal temperature for malaria transmission is dramatically lower than previously predicted. *Ecology Letters*, 16(1):22–30, 2013. DOI: 10.1111/ele.12015

[8] Nyawanda, B.O., Beloconi, A., Khagayi, S., et al. The relative effect of climate variability on malaria incidence after scale-up of interventions in western Kenya. *Parasite Epidemiology and Control*, 21:e00297, 2023. DOI: 10.1016/j.parepi.2023.e00297

[9] Beke, O.A.-H., Assi, S.-B., Kokrasset, A.P.H., et al. Implication of agricultural practices in the micro-geographic heterogeneity of malaria transmission in Bouna, Côte d'Ivoire. *Malaria Journal*, 22(1):310, 2023. DOI: 10.1186/s12936-023-04748-3

[10] Riebler, A., Sørbye, S.H., Simpson, D., & Rue, H. An intuitive Bayesian spatial model for disease mapping that accounts for scaling. *Statistical Methods in Medical Research*, 25(4):1145–1165, 2016. DOI: 10.1177/0962280216660421

[11] Simpson, D., Rue, H., Riebler, A., Martins, T.G., & Sørbye, S.H. Penalising model component complexity: a principled, practical approach to constructing priors. *Statistical Science*, 32(1):1–28, 2017. DOI: 10.1214/16-STS576

[12] Rue, H., Martino, S., & Chopin, N. Approximate Bayesian inference for latent Gaussian models by using integrated nested Laplace approximations. *Journal of the Royal Statistical Society: Series B*, 71(2):319–392, 2009. DOI: 10.1111/j.1467-9868.2008.00700.x

[13] Yamana, T.K., & Eltahir, E.A.B. Incorporating the effects of humidity in a mechanistic model of malaria transmission. *Proceedings of the National Academy of Sciences*, 110(46):18566–18570, 2013.

[14] Paaijmans, K.P., Wandago, M.O., Githeko, A.K., & Takken, W. Unexpected high losses of *Anopheles gambiae* larvae due to rainfall. *PLoS ONE*, 4(11):e7855, 2009.

[15] Okiring, J., Routledge, I., Epstein, A., et al. Associations between environmental covariates and temporal changes in malaria incidence in high transmission settings of Uganda. *BMC Public Health*, 21:1962, 2021. DOI: 10.1186/s12889-021-11949-5

[16] Nzabakiriraho, J.D., & Gayawan, E. Geostatistical modelling of malaria prevalence among under-five children in Rwanda. *BMC Public Health*, 21(1):369, 2021.

[17] Utazi, C.E., Thorley, J., Alegana, V.A., Ferrari, M.J., Takahashi, S., Metcalf, C.J.E., & Lessler, J. High-resolution mapping for public health. *Nature Communications*, 11:1–10, 2020.

[18] Bhatt, S., Weiss, D.J., Cameron, E., et al. The effect of malaria control on *Plasmodium falciparum* in Africa. *Nature*, 526:207–211, 2015.

[19] Siraj, A.S., Santos-Vega, M., Bouma, M.J., et al. Altitudinal changes in malaria incidence in highlands of Ethiopia and Colombia. *Science*, 343(6175):1154–1158, 2014.

[20] World Health Organisation. Climate-resilient health systems. WHO, Geneva, 2021.

[21] Rubuga, F.K., Moraga, P., Ahmed, A., Siddig, E., Remera, E., Moirano, G., Cissé, G., & Utzinger, J. Spatio-temporal dynamics of malaria in Rwanda between 2012 and 2022: a demography-specific analysis. *Infectious Diseases of Poverty*, 13(1):67, 2024. DOI: 10.1186/s40249-024-01237-w [PMC11403800]

[22] Uwimana, A., Legrand, E., Stokes, B.H., Ndikumana, J.-L.M., Warsame, M., Umulisa, N., Imwong, M., Mahmud, A., Birindabagabo, P., Tabaro, G., et al. Emergence and clonal expansion of in vitro artemisinin-resistant *Plasmodium falciparum* kelch13 R561H mutant parasites in Rwanda. *Nature Medicine*, 26:1602–1608, 2020. DOI: 10.1038/s41591-020-1005-2

[23] Uwimana, A., Umulisa, N., Venkatesan, M., Adjei, G.O., Barte-Bitterman, L., Bassat, Q., Bhatt, D., Bondosian, N., et al. Association of *Plasmodium falciparum* kelch13 R561H genotypes with delayed parasite clearance in Rwanda: an open-label, single-arm, multicentre, therapeutic efficacy study. *The Lancet Infectious Diseases*, 21(8):1120–1128, 2021. DOI: 10.1016/S1473-3099(21)00142-0

[24] Conrad, M.D., Asua, V., Garg, S., Giesbrecht, D., Niaré, K., Smith, S., Namuganga, J.F., Katairo, T., Legac, J., Crudale, R., Tumwebaze, P.K., et al. Evolution of partial resistance to artemisinins in malaria parasites in Uganda. *New England Journal of Medicine*, 389(8):722–732, 2023. DOI: 10.1056/NEJMoa2211803

[25] Accrombessi, M., Cook, J., Dangbenon, E., Yovogan, B., Akogbeto, M., Agossa, F., Sovi, A., Tokponnon, F., Atachi, T., Gnanguenon, V., et al. Efficacy of pyriproxyfen-pyrethroid long-lasting insecticidal nets compared with pyrethroid-only nets for malaria control in Benin: a cluster-randomised, superiority trial. *The Lancet*, 401(10371):435–446, 2023. DOI: 10.1016/S0140-6736(22)01882-0

[26] Semakula, M., Niragire, F., & Faes, C. Spatio-temporal Bayesian models for malaria risk using survey and health facility routine data in Rwanda. *International Journal of Environmental Research and Public Health*, 20(5):4283, 2023. DOI: 10.3390/ijerph20054283 [PMC10001932]